Amino Acids (2012) 42:831–841
DOI 10.1007/s00726-011-0999-7

ORIGINAL ARTICLE

The members of *Arabidopsis thaliana PAO* gene family exhibit distinct tissue- and organ-specific expression pattern during seedling growth and flower development

Paola Fincato · Panagiotis N. Moschou · Abdellah Ahou · Riccardo Angelini · Kalliopi A. Roubelakis-Angelakis · Rodolfo Federico · Paraskevi Tavladoraki

Received: 15 March 2011 / Accepted: 8 June 2011 / Published online: 4 August 2011

Abstract Polyamine oxidases (PAOs) are FAD-dependent enzymes involved in polyamine catabolism. In *Arabidopsis thaliana*, five PAOs (AtPAO1-5) are present with cytosolic or peroxisomal localization. Here, we present a detailed study of the expression pattern of *AtPAO1*, *AtPAO2*, *AtPAO3* and *AtPAO5* during seedling and flower growth and development through analysis of promoter activity in *AtPAO*::*β-glucuronidase* (*GUS*) transgenic *Arabidopsis* plants. The results reveal distinct expression patterns for each studied member of the *AtPAO* gene family. *AtPAO1* is mostly expressed in the transition region between the meristematic and the elongation zone of roots and anther tapetum, *AtPAO2* in the quiescent center, columella initials and pollen, *AtPAO3* in columella, guard cells and pollen, and *AtPAO5* in the vascular system of roots and hypocotyls. Furthermore, treatment with the plant hormone abscisic acid induced expression of *AtPAO1* in root tip and *AtPAO2* in guard cells. These data suggest distinct physiological role(s) for each member of the *AtPAO* gene family.

Keywords Polyamines · Polyamine oxidase · *Arabidopsis thaliana* · GUS · Guard cells · Pollen · Tapetum · Roots

Abbreviations

ABA	Abscisic acid
AtPAO	*Arabidopsis thaliana* polyamine oxidase
CuAOs	Copper-containing amine oxidases
GFP	Green fluorescent protein
GUS	*β*-Glucuronidase
HR	Hypersensitive response
MES	2-(*N*-morpholino) ethanesulfonic acid
MS	Murashige and Skoog
Nor-Spm	Norspermine
PAO	Polyamine oxidase
PCD	Programmed cell death
Put	Putrescine
ROS	Reactive oxygen species
SAM	Shoot apical meristem
SMO	Spermine oxidase
Spd	Spermidine
Spm	Spermine
Therm-Spm	Thermospermine
TMV	Tobacco mosaic virus
ZmPAO	Maize polyamine oxidase

Electronic supplementary material The online version of this article (doi:10.1007/s00726-011-0999-7) contains supplementary material, which is available to authorized users.

P. Fincato · A. Ahou · R. Angelini · R. Federico · P. Tavladoraki (✉)
Department of Biology, University 'ROMA TRE', Viale G. Marconi 446, 00146 Rome, Italy
e-mail: tavlador@uniroma3.it

P. N. Moschou · K. A. Roubelakis-Angelakis
Department of Biology, University of Crete, 714 09 Heraklion, Greece

Introduction

Polyamines are small aliphatic amines found in a wide range of organisms from bacteria to plants and animals. In plants, polyamines are involved in various physiological events, such as growth and development including

senescence, as well as stress responses (Kusano et al. 2008; Alcázar et al. 2010; Handa and Mattoo 2010). Putrescine (Put), spermidine (Spd) and spermine (Spm) are the most commonly found polyamines in higher plants and are present in free and conjugated soluble or insoluble forms. Soluble conjugated polyamines are covalently bound to small molecules, such as phenolic compounds, while insoluble conjugated polyamines are covalently bound to macromolecules such as nucleic acids and proteins. In addition to these standard polyamines, some other polyamines, as for example homospermidine, norspermine (Nor-Spm) and thermospermine (Therm-Spm), have been detected as minor components of cellular polyamine pools in several biological systems, including plants (Knott et al. 2007; Kakehi et al. 2008; Minguet et al. 2008; Naka et al. 2010; Oshima 2010; Vera-Sirera et al. 2010). In *Arabidopsis thaliana*, Therm-Spm, which is a structural isomer of Spm, is formed from Spd by Therm-Spm synthase, whose loss of function causes severe shortening of internodes, smaller mature leaves and over-proliferation of the xylem vessel elements in the vascular bundles of the inflorescence stems (Vera-Sirera et al. 2010).

Polyamines are catabolized by copper-containing amine oxidases (CuAOs) and FAD-dependent polyamine oxidases (PAOs). CuAOs catalyze the oxidation of Put at the primary amino group producing Δ^1-pyrroline, ammonia and H_2O_2, while PAOs catalyze the oxidation of Spm, Spd and/or their acetylated derivatives at the secondary amino groups (Angelini et al. 2010). The chemical identity of PAO-catalyzed reaction products depends on the enzyme source and reflects the mode of substrate oxidation. All the so-far characterized PAOs from monocotyledonous plants, such as the extracellular maize PAO (ZmPAO), are involved in the terminal catabolism of Spd and Spm producing 1,3-diaminopropane, H_2O_2 and an aminoaldehyde (Angelini et al. 2010; Marcocci et al. 2008), while the animal PAOs and Spm oxidases (SMO), as well as the four *Arabidopsis thaliana* PAOs characterized so far, are involved in a polyamine back-conversion pathway producing Spd and Put from the oxidation of Spm and Spd (or their acetyl-derivatives), respectively, together with H_2O_2 and aminopropanal (or 3-acetamidopropanal) (Tavladoraki et al. 2006, 2011; Casero and Marton 2007; Kamada-Nobusada et al. 2008; Moschou et al. 2008c; Amendola et al. 2009; Angelini et al. 2010; Fincato et al. 2010; Takahashi et al. 2010).

In *A. thaliana*, five PAO genes are present (*AtPAO1*-*AtPAO5*). AtPAO1, which has a predicted cytosolic localization and a similar gene organization to that of the extracellular ZmPAO, oxidizes preferentially Spm, Therm-Spm and Nor-Spm, but not Spd (Tavladoraki et al. 2006). AtPAO2, AtPAO3 and AtPAO4, which have a peroxisomal localization and form a distinct subfamily having similar gene structure and high sequence homology to each other (Fincato et al. 2010), oxidize both Spd and Spm (Moschou et al. 2008c; Kamada-Nobusada et al. 2008; Fincato et al. 2010; Takahashi et al. 2010). In particular, while AtPAO2 is equally active with Spm and Spd, AtPAO3 is twofold more active with Spd than with Spm, and AtPAO4 is tenfold more active with Spm than with Spd. AtPAO5, whose catalytic properties have not been determined yet, has a predicted cytosolic localization and a very different gene organization from that of the other *AtPAOs* and of *ZmPAO* (Fincato et al. 2010).

In an effort to elucidate the physiological roles of the members of the *AtPAO* gene family, we present herein the tissue/organ-specific expression pattern of *AtPAO1*, *AtPAO2*, *AtPAO3* and *AtPAO5* during seedling and flower growth and development through analysis of promoter activity in transgenic *Arabidopsis* plants expressing *AtPAO*::*β-glucuronidase* (*GUS*) constructs. Although more data could still be necessary to determine in detail the expression profile at the mRNA and protein level, the present study provides evidence for important differences in the spatial and temporal expression pattern of the various *AtPAOs*, which suggest distinct physiological roles for each member of the *AtPAO* gene family.

Experimental procedures

Plant material and growth conditions

Plants of *A. thaliana*, ecotype Columbia-0 (Col-0), were grown in a growth chamber at a temperature of 23°C, photoperiod of 16/8 h and relative humidity 55%. For in vitro growth, *A. thaliana* seeds were surface sterilized and sown on plates containing sterile ½ Murashige and Skoog (MS) medium (pH 5.7) supplemented with 2% (w/v) sucrose and solidified with 0.8% (w/v) agar. Seedlings 3–15 days old were analyzed for GUS activity. For abscisic acid (ABA) treatment, seedlings were grown for 6 days on solidified ½ MS medium (pH 5.7) supplemented with 0.5% (w/v) sucrose. Seedlings were then transferred into six-well tissue culture clusters containing 50 mM MES, pH 5.7. ABA was added at a final concentration of 10 μM and, after incubation for 4 h with shaking, seedlings were analyzed for GUS activity.

Construction of transgenic lines

To construct *AtPAO*::*GUS* transgenic plants for *AtPAO1* (At5g13700), *AtPAO2* (At2g43020), *AtPAO3* (At3g59050) and *AtPAO5* (At4g29720), promoter regions of 2.0–2.8 kb upstream of ATG were amplified from *A. thaliana* Col-0 genomic DNA by PCR, cloned into the pDONR207 vector

(Invitrogen) via Gateway technology (Invitrogen) and sequenced. *AtPAO2* and *AtPAO5* promoter regions were inserted upstream of the *GFP–GUS* fusion gene in the pKGWFS7 binary vector (Karimi et al. 2002), *AtPAO3* promoter region upstream of the *GUS* gene in the pGWB3 binary vector (Nakagawa et al. 2007) and *AtPAO1* promoter region upstream of the reporter genes in both the pKGWFS7 and the pGWB3 binary vectors. In particular, a promoter region of 2.0 kb was amplified for *AtPAO1* using the oligonucleotides *PromAtPAO1-for* (5′-GGGGACAAGTTTGTACAAAAAAGCAGGCTGCAGGCTGACTTCATGAAGATGCCATTC-3′) and *PromAtPAO1-rev* (5′-GGGGACCACTTTGTACAAGAAAGCTGGGTTAGAGAGAGAGCGAAAGGTGTTTGTTAG-3′) of 2.9 kb for *AtPAO2* using the oligonucleotides *PromAtPAO2-for* (5′-GGGGACAAGTTTGTACAAAAAAGCAGGCTCTTTGGGATGCAGTTTATTTTCTAATCAAAAC-3′) and *PromAtPAO2-rev* (5′-GGGGACCACTTTGTACAAGAAAGCTGGGTGATTTTTTTTTCAATTGATCAAACGATTACTCTC-3′), 2.0 kb for AtPAO3 using the oligonucleotides *PromAtPAO3-for* (5′-GGGGACAAGTTTGTACAAAAAAGCAGGCTTGGGAAGGAACAACAAAGAAAC-3′) and *PromAtPAO3-rev* (5′-GGGGACCACTTTGTACAAGAAAGCTGGGTACATGATTCAACAATGAACGGAG-3′) and 2.5 kb for *AtPAO5* using the oligonucleotides *PromAtPAO5-for* (5′-GGGGACAAGTTTGTACAAAAAAGCAGGCTGGTGGAAGGTTGCTCTTGTATATTATTTAGTGTTG-3′) and *PromAtPAO5-rev* (5′-GGGGACCACTTTGTACAAGAAAGCTGGGTAGTTAAAGGAATCTCCTTGTCGGTGTTGG-3′). The resulting *AtPAO*::*GUS* constructs were used to transform *A. thaliana* Col-0 wild-type plants by the *Agrobacterium tumefaciens* (strain C58C1)-mediated floral dip transformation method as described by Clough and Bent (1998). At least three independent transgenic lines per construct, selected by kanamycin resistance and PCR analysis, at T1, T2 and T3 generation were examined for GUS activity.

Histochemical GUS analysis

GUS staining of *AtPAO*::*GUS Arabidopsis* transgenic plants was performed essentially as described by Jefferson (1987). Briefly, seedlings were gently soaked in 90% (v/v) cold acetone for 1 h at −20°C for prefixation, rinsed with 50 mM sodium phosphate buffer of pH 7.0 and vacuum infiltrated in staining solution [1 mM 5-bromo-4-chloro-3-indolyl-*β*-D-glucuronide, 2.5 mM potassium ferrocyanide, 2.5 mM potassium ferricyanide, 0.2% (v/v) Triton X-100, 10 mM EDTA, 50 mM sodium phosphate buffer, pH 7.0]. The reaction was allowed to proceed at 37°C overnight or as otherwise indicated. Chlorophyll was extracted by several washings first with ethanol:acetic acid (3:1) and then with 70% (v/v) ethanol. To obtain longitudinal and transverse sections, GUS-stained seedlings and inflorescences were embedded in Technovit 7100 resin (Kulzer) and 20 μm sections were obtained using a Microm HM330 microtome. Images were acquired by a Leica DFC420 digital camera applied to an Olympus BX51 microscope.

Results

AtPAO expression pattern during seedling growth

To determine the physiological role(s) of each member of the *AtPAO* gene family and to verify whether the various *AtPAOs* have overlapping or distinct expression patterns, promoter activity was analyzed by GUS staining in transgenic *Arabidopsis* plants expressing *AtPAO*::*GUS* constructs. To this end, 2,000–2,900 bp promoter regions including the 5′-UTR of *AtPAO1*, *AtPAO2*, *AtPAO3* (the last two being chosen as representative members of the *AtPAO2-4* subfamily) and *AtPAO5* were amplified and fused to the coding region of the *GUS* gene alone and/or in fusion to *GFP* gene in the pGWB3 and pKGWFS7 binary vectors, respectively. As controlled through *AtPAO1* promoter analysis, data obtained from the two binary vectors are identical. Seedlings from *AtPAO*::*GUS* transgenic *Arabidopsis* plants were analyzed for GUS activity by histochemical analysis at various developmental stages. Comparative data using GFP as a reporter are not shown here due to problems of tissue autofluorescence and low GFP-specific signal.

In 2- to 5-day-old seedlings, *AtPAO1*-related GUS staining was present in root tips forming a characteristic blue spot in the transition region between the meristematic and the elongation zone (Figs. 1a, b, 2a). This spot mainly involved cortical tissues and often had unilateral distribution (Fig. 2b). Interestingly, the *AtPAO1*-related GUS staining in this region was increased following treatment with ABA (Figs. 3, S1). In 5- to 8-day-old seedlings, the *AtPAO1*-related GUS staining of roots was extended toward the maturation zone involving all tissues (Figs. 1c, 2c). In young seedlings, *AtPAO1*-related GUS staining was present in cotyledons (Fig. 1f), shoot apex (Fig. 1d, e) and newly emerging leaves (Fig. 1d), whereas no staining was observed in hypocotyls (Fig. 1a). Later in development, cotyledons and expanded leaves showed GUS staining at the tips and hydathodes, respectively (data not shown). Staining of stipules was observed as well (Fig. 1e).

AtPAO2-related GUS staining was present in the root apex of 2- to 5-day-old seedlings (Fig. 1g, h). In particular, *AtPAO2*-related GUS staining was localized near the quiescent center and in columella initials (Fig. 1h). Staining was also present in the elongation and differentiation zone of the roots up to the hypocotyl–root junction site involving

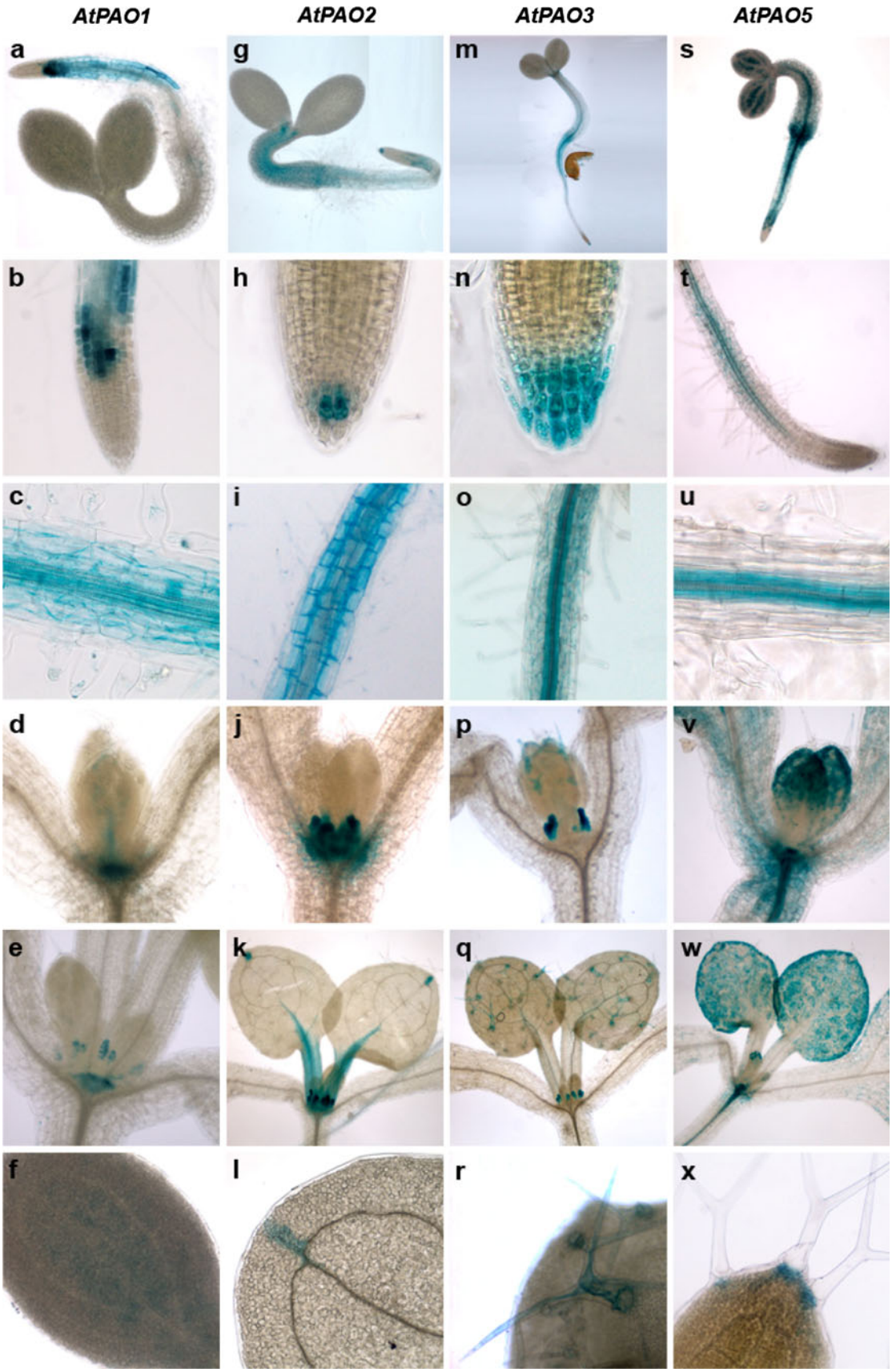
AtPAO1
AtPAO2
AtPAO3
AtPAO5
a
g
m
s
b
h
n
t
c
i
o
u
d
j
p
v
e
k
q
w
f
l
r
x

◀ **Fig. 1** *AtPAO1*, *AtPAO2*, *AtPAO3* and *AtPAO5* spatial expression pattern during seedling growth. *AtPAO*::*GUS* transgenic *A. thaliana* plants for the various *AtPAOs* were analyzed by GUS staining for *AtPAO1*, *AtPAO2, AtPAO3* and *AtPAO5* expression. Highly reproducible results were obtained from more than three independent transgenic lines

all tissues (Figs. 1i, 2d, e). This staining pattern in roots persisted during all the following developmental stages. In very young (2- to 3-day-old) seedlings, staining was observed in hypocotyls (Fig. 1g), which however disappeared later during plant development. No staining was detectable in cotyledons of young seedlings (Fig. 1g) and only later in development *AtPAO2*-related GUS staining appeared in the cotyledonary tips (Fig. 1l). In 5- to 8-day-old seedlings, strong *AtPAO2*-related GUS staining was observed in roots with a pattern similar to that observed at earlier developmental stages. At this developmental stage, staining at the shoot apical meristem (SAM) was found (Fig. 1j, k), which is consistent with *AtPAO2* expression in the meristematic cells of the root tip and in agreement with recently published data (Takahashi et al. 2010). In 5- to 8-day-old seedlings, staining at the stipules and newly expanding leaves was also observed (Fig. 1j, k). In the latter case, staining was mainly localized around the vascular tissues and in the petioles, and gradually diminished during leaf development in parallel with an increasing staining in leaf hydathodes (Fig. 1k). Staining of some guard cells was observed too and interestingly the number of GUS-stained guard cells was increased following treatment with ABA (Fig. 3).

In 2- to 5-day-old seedlings *AtPAO3*-related GUS staining was present in lateral root cap and columella (Fig. 1n). In addition, staining was present in the elongation and differentiation zones of the roots up to the hypocotyl–root junction site (Fig. 1o) involving epidermis, cortex, pericycle and the vascular system but not endodermis (Fig. 2f). Hypocotyls appeared stained in the region adjacent to the hypocotyl–root junction site (Figs. 1m, 2g). This expression pattern in roots and hypocotyls was also observed in 5- to 8-day-old seedlings. At this developmental stage, stipules, trichomes (Fig. 1p, q, r) and guard cells (Fig. 3) were stained too. Contrary to *AtPAO2*, treatment with ABA did not increase staining of guard cells (Fig. 3).

In 2- to 5-day-old seedlings, *AtPAO5*-related GUS staining was present in roots, hypocotyls and cotyledons (Fig. 1s) in agreement with microarray data (*Arabidopsis* eFP Browser, TAIR). In the roots, the staining was extended from the hypocotyl–root junction region up to the transition region between the elongation and the meristematic zones and was absent from the root cap (Fig. 1t). This *AtPAO5*-related GUS staining of the roots involved the vascular tissue plus the pericycle (Figs. 1u, 2h). In hypocotyls, staining was observed from the shoot apex to the hypocotyl–root junction, involving the stele (Figs. 1s, 2i). In cotyledons, a rather diffused staining was observed (Fig. 1s). In 5- to 8-day-old seedlings, staining in hypocotyls, cotyledons and roots persisted. At this developmental stage, *AtPAO5*-related GUS staining also appeared at the distal ends of newly emerging leaves (Fig. 1v), which was extended to the whole leaf area as leaf development proceeded (Fig. 1w). Moreover, staining was observed in the base of the trichomes (Fig. 1x). Later during development, staining in hypocotyls, cotyledons and leaves appeared reduced (data not shown).

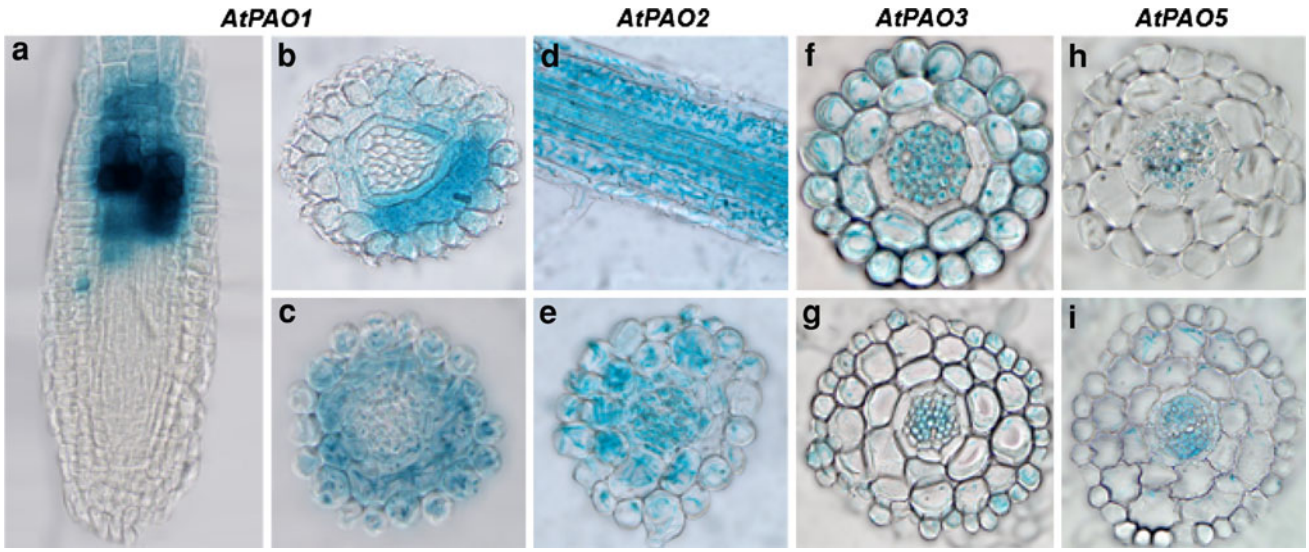

Fig. 2 Cross sections of *AtPAO*::*GUS* transgenic *A. thaliana* plants. Longitudinal (**a**, **d**) and transversal (**b**, **c**, **e**–**i**) sections of roots (**a**–**f**, **h**) and hypocotyls (**g**, **i**) obtained after GUS staining are shown

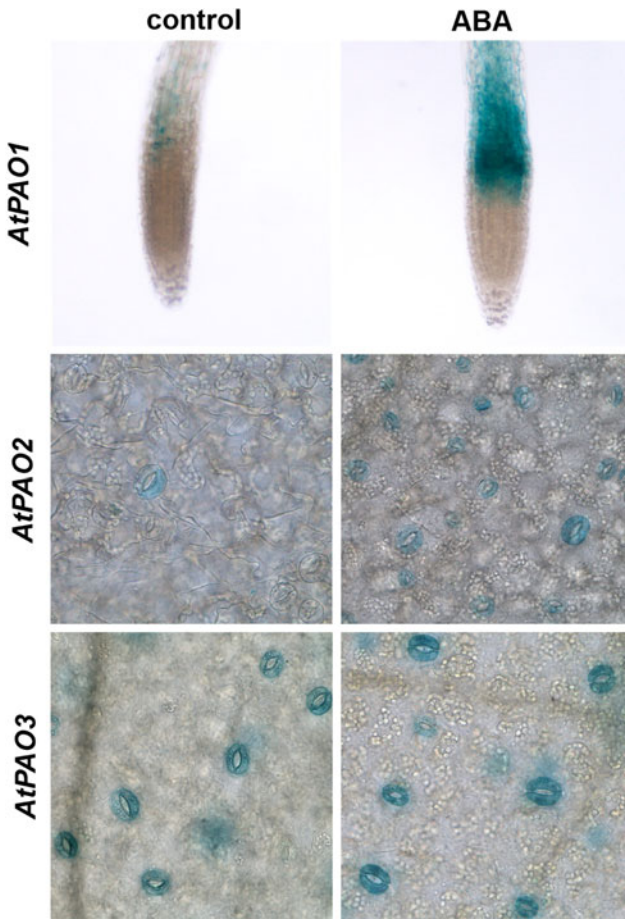

Fig. 3 ABA-inducible expression of *AtPAO1* and *AtPAO2*. *AtPAO*::*GUS* transgenic *Arabidopsis* plants were treated or not with 10 µM ABA for 4 h and then analyzed for GUS activity. The color reaction was allowed to proceed for 30 min (*AtPAO1*) or overnight (*AtPAO2* and *AtPAO3*). Representative plants are shown. The experiment was repeated three times ($n > 10$)

AtPAO promoter activity in flowers

When *A. thaliana* inflorescences at different developmental stages were screened for *AtPAO1* expression, a strong *AtPAO1*-related GUS signal was observed in very young, completely closed flower buds (Fig. 4a, b). A close-up of stained buds revealed that GUS staining was localized in the anthers (Fig. 4c, d) and in particular in the microspores and the tapetum (Figs. 4d, 5a, b). Microspore staining was gradually decreased during flower development (Fig. 5a, b), being very high in pollen mother cells (Fig. 5a) and not at all evident in mature pollen grains (Fig. 4e), contrary to microarray data which report *AtPAO1* expression in pollen grains (*Arabidopsis* eFP Browser, TAIR). Anther staining was finally restricted to the anther–filament junction (Fig. 4e). *AtPAO1*-related GUS staining appeared also in receptacle and stem, involving mainly vascular tissues (Fig. 4a, b). This staining gradually diminished during flower development. No signal was observed in pistils, petals, sepals, silique or seeds (data not shown).

Fig. 4 *AtPAO1*, *AtPAO2*, *AtPAO3* and *AtPAO5* spatial expression pattern during flower development. *AtPAO*::*GUS* transgenic *A. thaliana* plants for the various AtPAOs were analyzed by GUS staining. Analysis was performed in more than three independent transgenic lines obtaining highly reproducible results ▶

AtPAO2-related GUS staining was present very early during flower development (Fig. 4g). As flower development proceeded and before pollen maturation, strong staining appeared in pistils (stigma and ovary wall; Figs. 4h, 5c, d), which gradually decreased and finally disappeared (Fig. 4f). Mature pollen grains were stained as well, in agreement with microarray data (*Arabidopsis* eFP Browser, TAIR). Interestingly, this staining persisted during pollination and pollen tube growth (Fig. 4j, k). No *AtPAO2*-related staining was present in petals, sepals, receptacles, stems, siliques or seeds (data not shown).

AtPAO3-related GUS staining was present in very young flower buds. Later during flower development, pistils and anthers were stained (Fig. 4l). In particular, in young flowers *AtPAO3*-related GUS staining was present in pistil walls and septum (Figs. 4n, 5e, f). Anther filaments and pollen grains were stained too (Fig. 4o) in accordance with microarray data (*Arabidopsis* eFP Browser, TAIR). Similarly to *AtPAO2*, pollen staining persisted during pollination and pollen tube growth (Fig. 4p, q). Nectars (Fig. 4l) and guard cells of sepals (Fig. 4m) were also stained.

For *AtPAO5*, GUS staining was observed already in very young, completely closed flower buds (Fig. 4r). A close-up of stained buds showed staining localization in the anthers (Fig. 4u) and in particular in anther tapetal cells (Fig. 5g, h) as in the case of *AtPAO1*. This coloration was gradually reduced during flower development and finally it was localized in the anther–filament junction site, similarly to *AtPAO1*, and in the upper part of the filament (Fig. 4v). *AtPAO5*-related staining was also observed in sepals, petals and pistils (Fig. 4r), but not in pollen grains. Pistils were stained in the stigma and in the septum before pollination (Fig. 4r, t), whereas after pollination pistil staining drastically decreased (Fig. 4w). Receptacles were strongly stained from the early stages of flower development to silique formation (Fig. 4r, s), whereas siliques and seeds were not stained.

Discussion

Cellular homeostasis of polyamines is tightly controlled via polyamine sequestration, and/or via regulation of the biosynthetic and/or the catabolic genes. However, polyamine catabolism seems to be more than a biochemical process

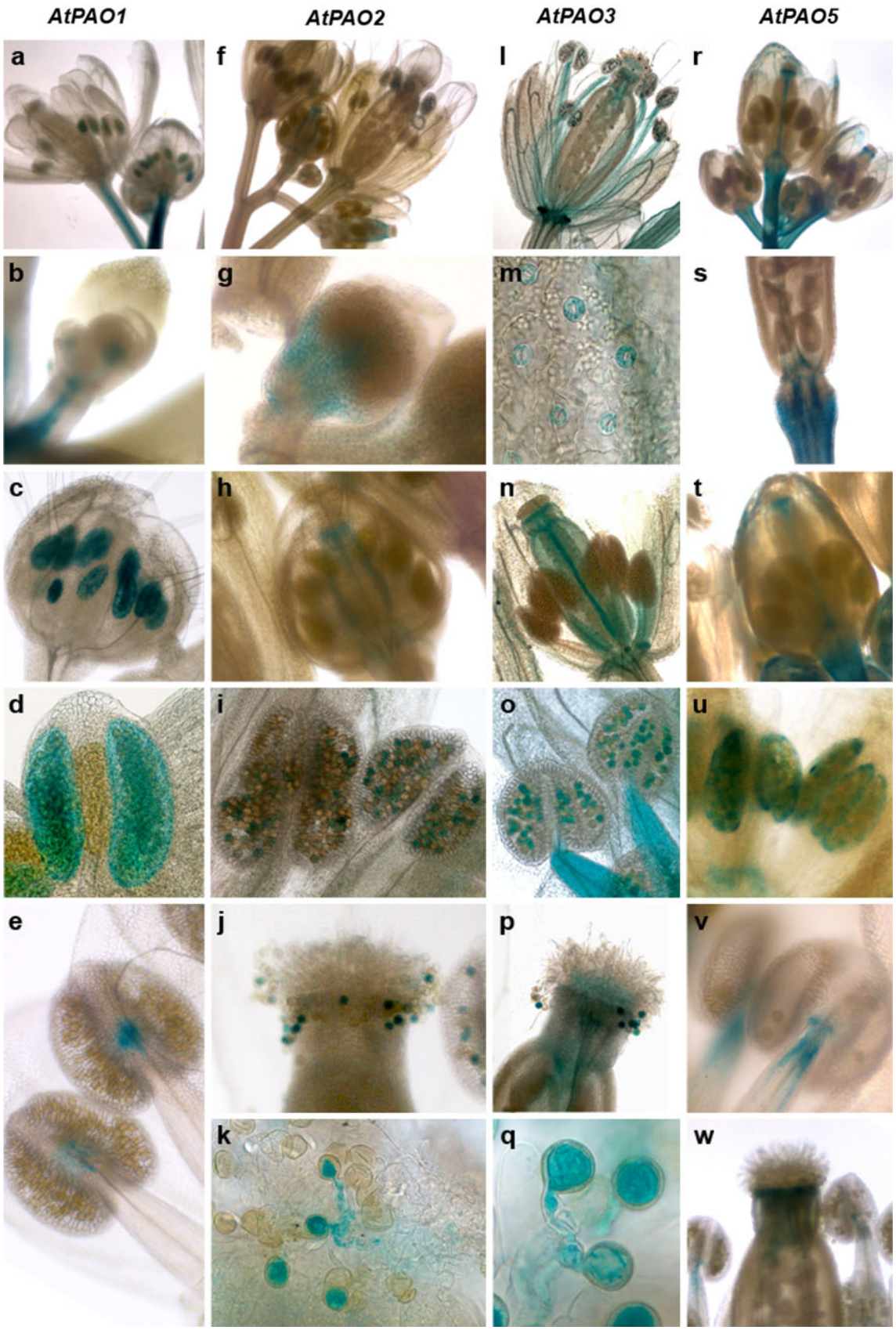
AtPAO1
AtPAO2
AtPAO3
AtPAO5
a
f
l
r
b
g
m
s
c
h
n
t
d
i
o
u
e
j
p
v
k
q
w

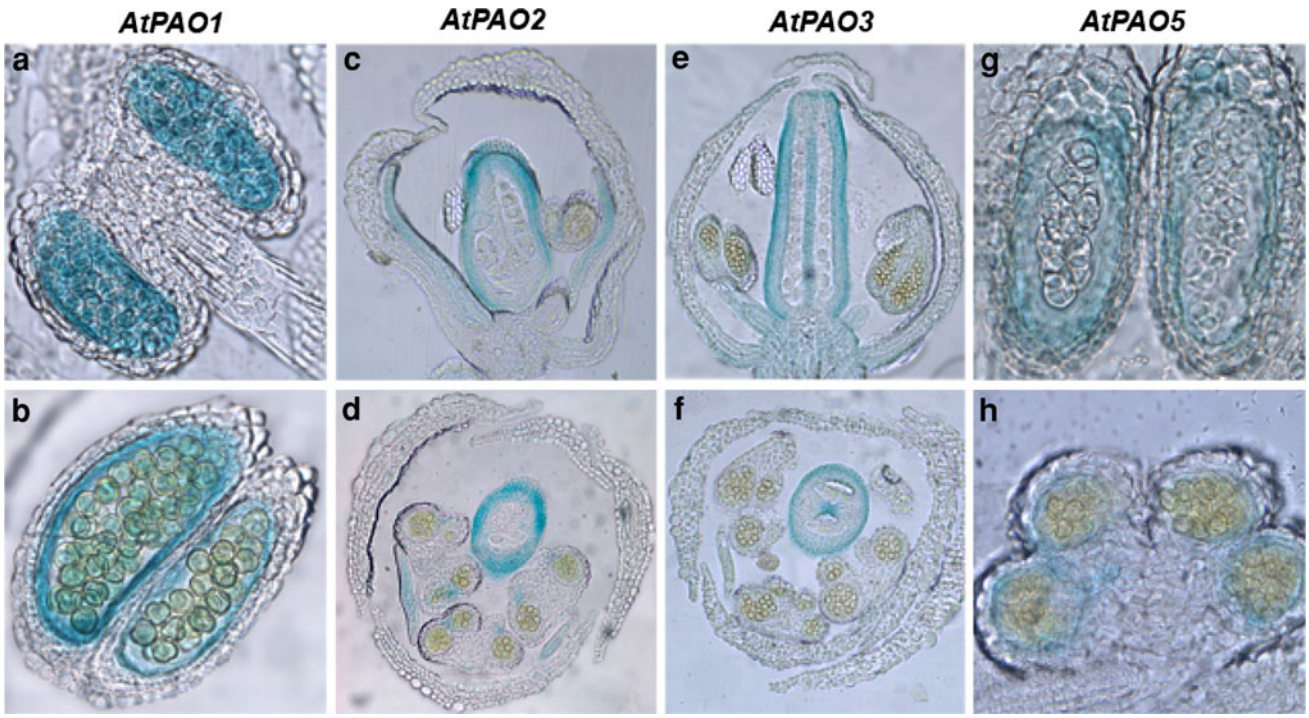

Fig. 5 Cross sections of flowers from *AtPAO*::*GUS* transgenic *A. thaliana* plants obtained after GUS staining

aiming to control polyamine homeostasis in plants. Indeed, the H_2O_2 produced by polyamine catabolism participates in the signaling network; depending on its levels, it signals events important in different developmental processes, i.e., the programmed cell death syndrome (PCD) and pollen tube elongation, as well as in defense responses to biotic and abiotic stresses (Yoda et al. 2003, 2006; Marina et al. 2008; Moschou et al. 2008a, b, c, 2009; Angelini et al. 2010; Wu et al. 2010). Furthermore, H_2O_2 production by extracellular CuAO and PAO has been shown to be involved in peroxidase-mediated synthesis of suberin and lignin taking place during cell wall maturation in the course of plant development as well as during wound healing and cell wall strengthening following pathogen attack (Angelini et al. 2010). Furthermore, Yoda et al. (2003, 2006) reported that Spd and Put accumulation and *PAO* expression increase in the extracellular space of *Nicotiana tabacum* cells exhibiting tobacco mosaic virus (TMV)-induced hypersensitive response (HR). Interestingly, they further showed that the cell death caused by TMV infection or cryptogein, an oomycete-originated elicitor, was partially mediated by H_2O_2 generated through polyamine catabolism in the extracellular space. Furthermore, Takahashi et al. (2003) provided evidence correlating Spm oxidation in the apoplast to induction of HR-associated defense-related genes. Polyamine catabolism in the extracellular space was also shown to be involved in defense responses against various necrotrophic and biotrophic pathogens (Marina et al. 2008; Moschou et al. 2009; Angelini et al. 2010). On the other hand, it has been reported that abiotic stress induces Spd exodous into the apoplast where it is oxidized by apoplastic PAO generating H_2O_2 (Moschou et al. 2008b). These data taken together reveal that in plants, the extracellular PAOs constitute a nodal point under specific abiotic and biotic stress conditions giving rise to increased apoplastic H_2O_2, which signals primary and secondary defense responses. In contrast to the so far characterized apoplastic PAOs which are involved in a terminal catabolic pathway, little is known until now of the physiological role(s) of the intracellular PAOs, as for example of the cytosolic AtPAO1 and AtPAO5 and the peroxisomal AtPAO2, AtPAO3 and AtPAO4, which are involved in a polyamine back-conversion pathway. In an attempt to elucidate these roles, we analyzed the *AtPAO1*, *AtPAO2*, *AtPAO3* and *AtPAO5* expression pattern during seedling and flower growth and development using *AtPAO*::*GUS* transgenic plants.

The results reported herein reveal a distinct expression pattern for each member of the *AtPAO* gene family. In particular, *AtPAO1* is highly expressed in the transition region between the meristematic and the elongation zone of the root (Fig. 1a, b), while *AtPAO2* and *AtPAO3* are expressed in the root cap (Fig. 1h, n). Interestingly, at the root cap differences exist between *AtPAO2* and *AtPAO3*, although they belong to the same PAO subfamily (Fincato et al. 2010). While *AtPAO2* is expressed only near the quiescent center and columella initials, *AtPAO3* is expressed in the lateral root cap and the whole columella

(Fig. 1h, n). Furthermore, while all four genes are expressed in the maturation zone of the roots, *AtPAO5* is specifically expressed in the vascular system of this zone (Figs. 1u, 2h), the other three being present both in vascular and cortical tissues (Figs. 1c, i, o, 2b, e, f).

All four *AtPAOs* analyzed exhibit distinct expression patterns also in the aerial part of the plant; *AtPAO1* and *AtPAO2* are specifically expressed in the SAM, the stipules and the leaf hydathodes (Fig. 1d, e, j, k), *AtPAO3* in the stipules (Fig. 1p, q), trichomes (Fig. 1r, q) and guard cells (Fig. 3), and *AtPAO5* in the vascular system of the hypocotyl and the base of the trichomes (Fig. 1s, x). In inflorescences, *AtPAO1* seems to be specifically expressed in the microspores and the tapetum (Figs. 4c, d, 5a, b), while *AtPAO2* and *AtPAO3* are specifically expressed in pistils (Fig. 4h, n) and pollen grains (Fig. 4i, o). *AtPAO5* exhibits an overlapping expression pattern with that of *AtPAO1*, *AtPAO2* and *AtPAO3* with some differences. In particular, although *AtPAO5* is initially expressed in anther tapetal cells (Figs. 4u, 5h) and then in the anther–filament junction site (Fig. 4v) similarly to *AtPAO1*, *AtPAO5* is also expressed in the upper part of the filament (Fig. 4v), in sepals and in petals (Fig. 4r) where *AtPAO1* expression is not found. In addition, similarly to *AtPAO2* and *AtPAO3*, *AtPAO5* is expressed only in the stigma and the septum and not in the ovary wall (Fig. 4r, t) as do *AtPAO2* and *AtPAO3* (Fig. 4h, n). Furthermore, *AtPAO5* is not expressed in pollen grains, in contrast to *AtPAO2* and *AtPAO3*. All these data together support different physiological role(s) of each of the members of the *AtPAO* gene family.

The *AtPAO2* and *AtPAO3* expression in pollen grains, an expression which persists during pollination and pollen tube growth, is consistent with recent results showing that in *A. thaliana*, H_2O_2 produced by PAO-mediated Spd oxidation triggers the opening of hyperpolarization-activated Ca^{2+}-permeable channels in pollen, thereby regulating pollen tube growth (Wu et al. 2010). Indeed, in pollen from *atpao3* loss-of-function mutants, the activation of Ca^{2+} currents by Spd was significantly disrupted resulting in reduced pollen tube growth and seed number (Wu et al. 2010).

AtPAO1 and *AtPAO5* expression in the tapetum (Fig. 5) is of great interest, since during maturation of stamens this tissue is characterized by the production and secretion of large quantities of proteins and a complex array of small metabolites essential for maturation and differentiation of the pollen grains. Following maturation of the pollen grains, the tapetum is lysed and undergoes PCD releasing the materials necessary for the formation of the pollen cell wall, which displays a high degree of mechanical resistance and is structurally the most complex type of plant cell wall. The exact role of *AtPAO1* and *AtPAO5* in these steps of flower development is not clear yet. They may have a role in stamen maturation through their reaction products (as for example H_2O_2, which as described above, is a well-known inducer of PCD) and/or regulation of polyamine levels. Indeed, both free and conjugated polyamines have been shown to be involved in flower development (Rastogi and Sawhney 1990). Interestingly, genes involved in the production of conjugated Spd have been recently shown to be specifically expressed in anther tapetum cells, while RNAi plants and knockout mutants presented alterations in pollen grains and impaired silique development (Fellenberg et al. 2008; Grienenberger et al. 2009).

ABA plays a pivotal role in the response of plants to abiotic stresses, including drought, salinity and cold, acting as a key regulator of stomatal apertures to restrict transpiration and reduce water loss. Several components are involved in the ABA signaling network, among which reactive oxygen species (ROS) are important second messengers. In *A. thaliana*, two plasma membrane-associated NADPH oxidases (AtrbohD and AtrbohF) are implicated in ABA-induced production of ROS in guard cells (Kwak et al. 2003), and in *Vicia faba* a CuAO is an essential enzymatic source for H_2O_2 production in ABA-induced stomatal closure via Put oxidation (An et al. 2008). Thus, the ABA-inducible *AtPAO2* expression in guard cells may suggest a role of this enzyme in the generation of H_2O_2 for the control of stomata closure/aperture. However, a role of *AtPAO2* in the ABA-inducible modulation of stomatal apertures through regulation of polyamine homeostasis is also possible. Indeed, it was shown that polyamines modulate stomatal aperture through a direct effect on the voltage-dependent inward K^+ channel in the plasma membrane of the guard cells (Liu et al. 2000). On the other hand, the ABA-inducible expression of *AtPAO2* implies a role of this enzyme in plant responses to abiotic stresses. An ABA-dependent environmental stress-inducible expression was also observed for other genes involved in polyamine metabolism, as for example for an arginine decarboxylase gene, an Spd synthase gene and an Spm synthase gene (Alcázar et al. 2010). Furthermore, Toumi et al. (2010) reported that ABA signals the reorientation of polyamine metabolism to regulate the generation of H_2O_2, which further signals stress responses. Further work will exploit the physiological significance of ABA-inducible *AtPAO2* expression in the guard cells (Fig. 3) and the physiological role(s) of *AtPAO2* and AtPAO3, the latter being constitutively expressed in the guard cells, stomata opening/closure and stress tolerance. Importantly, these studies on the peroxisomal AtPAOs could reveal the participation of peroxisomal metabolic pathways in important plant physiological processes, such as the control of stomata opening and defense responses.

The ABA-inducible specific expression pattern of *AtPAO1* in the transition region between the meristematic

and the elongation zones of the roots (Fig. 3) is very interesting and needs a detailed analysis to determine its physiological significance, taking into consideration that in roots polyamines have an important role in the regulation of ion channels under salt stress conditions (Zhao et al. 2007). Similarly, the *AtPAO2* and *AtPAO3* expression in the root tip as well as the *AtPAO5* expression in the vascular system of roots and hypocotyls necessitate further studies.

In conclusion, the comparative data presented herein on the expression pattern of the various *AtPAOs* suggest functional diversity inside the *A. thaliana PAO* gene family, in line with previous results from biochemical studies (Fincato et al. 2010). These data could be used as a guide for unraveling the physiological roles of the polyamine catabolic pathways in plant growth and development.

Acknowledgments We wish to thank Dr. Lucia Pomettini for technical assistance and Prof. Maria Maddalena Altamura for useful discussions. We are also grateful to Plants Systems Biology (University of Gent) for the kind gift of the pKGWFS7 binary vector. This work was supported by the University 'Roma Tre', the Italian Ministry of University and Research (PRIN 2005 and PRIN 2007) and implemented in the frame of COST FA605 Action.

References

Alcázar R, Altabella T, Marco F, Bortolotti C, Reymond M, Koncz C, Carrasco P, Tiburcio AF (2010) Polyamines: molecules with regulatory functions in plant abiotic stress tolerance. Planta 231:1237–1249

Amendola R, Cervelli M, Fratini E, Polticelli F, Sallustio DE, Mariottini P (2009) Spermine metabolism and anticancer therapy. Curr Cancer Drug Targets 9:118–130

An Z, Jing W, Liu Y, Zhang W (2008) Hydrogen peroxide generated by copper amine oxidase is involved in abscisic acid-induced stomatal closure in *Vicia faba*. J Exp Bot 59:815–825

Angelini R, Cona A, Federico R, Fincato P, Tavladoraki P, Tisi A (2010) Plant amine oxidases "on the move": an update. Plant Physiol Biochem 48:560–564

Casero RA Jr, Marton LJ (2007) Targeting polyamine metabolism and function in cancer and other hyperproliferative diseases. Nat Rev Drug Discov 6:373–390

Clough SJ, Bent AF (1998) Floral dip: a simplified method for *Agrobacterium*-mediated transformation of *Arabidopsis thaliana*. Plant J 16:735–743

Fellenberg C, Milkowski C, Hause B, Lange PR, Böttcher C, Schmidt J, Vogt T (2008) Tapetum-specific location of a cation-dependent *O*-methyltransferase in *Arabidopsis thaliana*. Plant J 56:132–145

Fincato P, Moschou PN, Spedaletti V, Tavazza R, Angelini R, Federico R, Roubelakis-Angelakis KA, Tavladoraki P (2010) Functional diversity inside the *Arabidopsis* polyamine oxidase gene family. J Exp Bot 62:1155–1168

Grienenberger E, Besseau S, Geoffroy P, Debayle D, Heintz D, Lapierre C, Pollet B, Heitz T, Legrand M (2009) A BAHD acyltransferase is expressed in the tapetum of *Arabidopsis* anthers and is involved in the synthesis of hydroxycinnamoyl spermidines. Plant J 58:246–259

Handa AK, Mattoo AK (2010) Differential and functional interactions emphasize the multiple roles of polyamines in plants. Plant Physiol Biochem 48:540–546

Jefferson RA (1987) Assaying chimeric genes in plants: the GUS gene fusion system. Plant Mol Biol Rep 5:387–405

Kakehi J, Kuwashiro Y, Niitsu M, Takahashi T (2008) Thermospermine is required for stem elongation in *Arabidopsis thaliana*. Plant Cell Physiol 49:1342–1349

Kamada-Nobusada T, Hayashi M, Fukazawa M, Sakakibara H, Nishimura M (2008) A putative peroxisomal polyamine oxidase, AtPAO4, is involved in polyamine catabolism in *Arabidopsis thaliana*. Plant Cell Physiol 49:1272–1282

Karimi M, Inzé D, Depicker A (2002) GATEWAY vectors for *Agrobacterium*-mediated plant transformation. Trends Plant Sci 7:193–195

Knott JM, Römer P, Sumper M (2007) Putative spermine synthases from *Thalassiosira pseudonana* and *Arabidopsis thaliana* synthesize thermospermine rather than spermine. FEBS Lett 581:3081–3086

Kusano T, Berberich T, Tateda C, Takahashi Y (2008) Polyamines: essential factors for growth and survival. Planta 228:367–381

Kwak JM, Mori IC, Pei ZM, Leonhardt N, Torres MA, Dangl JL, Bloom RE, Bodde S, Jones JD, Schroeder JI (2003) NADPH oxidase *AtrbohD* and *AtrbohF* genes function in ROS-dependent ABA signaling in *Arabidopsis*. EMBO J 22:2623–2633

Liu K, Fu H, Bei Q, Luan S (2000) Inward potassium channel in guard cells as a target for polyamine regulation of stomatal movements. Plant Physiol 124:1315–1326

Marcocci L, Casadei M, Faso C, Antoccia A, Stano P, Leone S, Mondovì B, Federico R, Tavladoraki P (2008) Inducible expression of maize polyamine oxidase in the nucleus of MCF-7 human breast cancer cells confers sensitivity to etoposide. Amino Acids 34:403–412

Marina M, Maiale SJ, Rossi FR, Romero MF, Rivas EI, Gárriz A, Ruiz OA, Pieckenstain FL (2008) Apoplastic polyamine oxidation plays different roles in local responses of tobacco to infection by the necrotrophic fungus *Sclerotinia sclerotiorum* and the biotrophic bacterium *Pseudomonas viridiflava*. Plant Physiol 147:2164–2178

Minguet EG, Vera-Sirera F, Marina A, Carbonell J, Blázquez MA (2008) Evolutionary diversification in polyamine biosynthesis. Mol Biol Evol 25:2119–2128

Moschou PN, Delis ID, Paschalidis KA, Roubelakis-Angelakis KA (2008a) Transgenic tobacco plants overexpressing polyamine oxidase are not able to cope with oxidative burst generated by abiotic factors. Physiol Plant 133:140–156

Moschou PN, Paschalidis KA, Delis ID, Andriopoulou AH, Lagiotis GD, Yakoumakis DI, Roubelakis-Angelakis KA (2008b) Spermidine exodus and oxidation in the apoplast induced by abiotic stress is responsible for H_2O_2 signatures that direct tolerance responses in tobacco. Plant Cell 20:1708–1724

Moschou PN, Sanmartin M, Andriopoulou AH, Rojo E, Sanchez-Serrano JJ, Roubelakis-Angelakis KA (2008c) Bridging the gap between plant and mammalian polyamine catabolism: a novel peroxisomal polyamine oxidase responsible for a full back-conversion pathway in *Arabidopsis*. Plant Physiol 47:1845–1857

Moschou PN, Sarris PF, Skandalis N, Andriopoulou AH, Paschalidis KA, Panopoulos NJ, Roubelakis-Angelakis KA (2009) Engineered polyamine catabolism preinduces tolerance of tobacco to bacteria and oomycetes. Plant Physiol 149:1970–1981

Naka Y, Watanabe K, Sagor GHM, Niitsu M, Pillai AM, Kusano T, Takahashi Y (2010) Quantitative analysis of plant polyamines including thermospermine during growth and salinity stress. Plant Physiol Biochem 48:527–533

Nakagawa T, Kurose T, Hino T, Tanaka K, Kawamukai M, Niwa Y, Toyooka K, Matsuoka K, Jinbo T, Kimura T (2007)

Development of series of gateway binary vectors, pGWBs, for realizing efficient construction of fusion genes for plant transformation. J Biosci Bioeng 104:34–41

Oshima T (2010) Enigmas of biosyntheses of unusual polyamines in an extreme thermophile, *Thermus thermophilus*. Plant Physiol Biochem 48:521–526

Rastogi R, Sawhney VK (1990) Polyamines and flower development in the male sterile stamenless-2 mutant of tomato (*Lycopersicon esculentum* Mill.). Plant Physiol 93:439–445

Takahashi Y, Berberich T, Miyazaki A, Seo S, Ohashi Y, Kusano T (2003) Spermine signalling in tobacco: activation of mitogen-activated protein kinases by spermine is mediated through mitochondrial dysfunction. Plant J 36:820–829

Takahashi Y, Cong R, Sagor GH, Niitsu M, Berberich T, Kusano T (2010) Characterization of five polyamine oxidase isoforms in *Arabidopsis thaliana*. Plant Cell Rep 29:955–965

Tavladoraki P, Rossi MN, Saccuti G, Perez-Amador MA, Polticelli F, Angelini R, Federico R (2006) Heterologous expression and biochemical characterization of a polyamine oxidase from *Arabidopsis* involved in polyamine back-conversion. Plant Physiol 141:1519–1532

Tavladoraki P, Cervelli M, Antonangeli F, Minervini G, Stano P, Federico R, Mariottini P, Polticelli F (2011) Probing mammalian spermine oxidase enzyme–substrate complex through molecular modeling, site-directed mutagenesis and biochemical characterization. Amino Acids 40:1115–1126

Toumi I, Moschou PN, Paschalidis KA, Daldoul S, Bouamama B, Chenennaoui S, Ghorbel A, Mliki A, Roubelakis-Angelakis KA (2010) Abscisic acid signals reorientation of polyamine metabolism to orchestrate stress responses via the polyamine exodus pathway in grapevine. J Plant Physiol 167:519–525

Vera-Sirera F, Minguet EG, Singh SK, Ljung K, Tuominen H, Blázquez MA, Carbonell J (2010) Role of polyamines in plant vascular development. Plant Physiol Biochem 48:534–539

Wu J, Qu H, Shang Z, Jiang X, Moschou PN, Roubelakis-Angelakis KA, Zhang S (2010) Spermidine oxidase derived H_2O_2 regulates pollen plasma membrane hyperpolarization-activated Ca^{2+}-permeable channels and pollen tube growth. Plant J 63:1042–1053

Yoda H, Yamaguchi Y, Sano H (2003) Induction of hypersensitive cell death by hydrogen peroxide produced through polyamine degradation in tobacco plants. Plant Physiol 132:1973–1981

Yoda H, Hiroi Y, Sano H (2006) Polyamine oxidase is one of the key elements for oxidative burst to induce programmed cell death in tobacco cultured cells. Plant Physiol 142:193–206

Zhao F, Song CP, He J, Zhu H (2007) Polyamines improve K^+/Na^+ homeostasis in barley seedlings by regulating root ion channel activities. Plant Physiol 145:1061–1072